Volume 16, Number 2, 2023. pp. 207-214

Jordan Journal of Physics

ARTICLE

Gamma-ray Spectrometry and X-ray Fluorescence Analysis for Natural Radioactivity Evaluation Associated with Radiation Hazard in Construction Materials

S. Boukhalfa and **R. Khelifi**

LPTHIRM, Department of Physics, Faculty of Sciences, University of Blida 1 Soumaa Street, BP 270, Blida (09000), Algeria.

Doi: **https://doi.org/10.47011/16.2.8**

Received on: 30/08/2021; *Accepted on: 10/11/2021*

Abstract: This paper had threefold objectives: 1) to evaluate the natural radioactivity using the gamma spectrometry technique, 2) to correct the gamma self-absorption using the transmission method, and 3) to perform mineralogical analysis using the X-ray fluorescence (XRF) analyzer in seven different types of construction materials. The transmission method was used to measure the linear attenuation coefficient μ(E) of the samples as well as their standards at different energetic points. Next, the μ(E) coefficients were used to calculate the self-absorption correction factors (C_{auto}), and then they were introduced in a simplified formula to correct the fraction of the attenuated gamma radiation inside the traveled medium. Moreover, the quantitative assessment of natural radioactive elements (^{238}U, ^{232}Th, and ^{40}K) was done in different geological matrices. The results have shown that the mean absorbed dose and the annual average dose received by these materials are 40.65 $nGy.h^{-1}$and 0.2 $mSv.y^{-1}$, respectively. According to the United Nations Scientific Committee on the Effects of Atomic Radiation (UNSCEAR), the obtained values in no way pose a risk to human health. For compositional analysis, the X-ray fluorescence (XRF) analyzer was used to determine the concentrations of the major oxides (SiO_2, CaO, CO_2, and Al_2O_3) along with other oxides in all collected samples. The compositional results show that the self-absorption correction factors varied depending on the density and chemical composition of a sample. The XRF data shows that the mineralogical compositions are within their recommended limit. Thus, from a health safety perspective, the composition of the minerals does not pose any significant risks.

Keywords: Gamma Spectrometry, Natural Radioactivity, Construction Materials, Radiological Hazard, Self-Absorption.

PACS NaI(Tl): Sodium iodide (NaI) detector activated by thallium (Tl), XRF: X-Ray Fluorescence.

1. Introduction

For centuries, construction materials have been commonly employed in the building of various structures, including underground tunnels, temples, bridges, etc. These materials can be used either in their natural state or transformed through industrial processes, which may involve the addition and/or mixing of other industrial products.

In the 1950s, the UNSCEAR and the ICRP reports revealed that the risk associated with exposure to ionizing radiation depends on different radioactive sources. They demonstrated that the principal dose received by human bodies is caused by external and internal exposure to naturally occurring radioactive materials

Corresponding Author: S. Boukhalfa **Email**: boukhalfasalma@gmail.com

(NORM) [1]. These materials can be found in food, water, air, and construction materials [2].

Following these reports, nuclear techniques were employed to evaluate the presence and potential radiological impact of NORM, as well as to assess any associated hazards for human safety.

Gamma-ray spectrometry is a widely employed technique for environmental measurements, offering a multi-elemental and quantitative approach that can be used for both laboratory-based and in situ measurements.

To accurately determine the concentrations of ^{40}K, ^{238}U, and ^{232}Th in a sample, various factors, such as sample nature, soil geology, chemical composition, density, and container geometry, have to be taken into account. These factors can introduce variations in the measured concentrations and require correction to obtain accurate values expressed in $Bq.kg^{-1}$ [3-4]. Besides this, the measured activities must be normalized by the self-attenuation correction factors (C_{auto}). Two different methods can be used to determine the C_{auto} factor, namely citing the transmission [5-9] and the Monte Carlo [10] methods. Cutshall et al. (2002) determined the C_{auto} factors and concluded that the sample mineralogy is relatively dependent on the self-absorption phenomenon.

The objectives of the present study are (i) the assessment of the radiological parameters of NORM, (ii) the auto-absorption correction of seven different types of construction materials, and (iii) the evaluation of any relation between the NORM concentration, chemical characteristics, and incident photon energy.

2. Materials and Methods

2.1 Sampling and Preparation

The investigated samples are cement, brick, concrete, sand, gravel, tuff, and floor tile. For the reason of anonymity, the collection was done at construction sites. To ensure the removal of any water content, these materials were air-dried in an oven at 100°C for 24 hours. Then, they were grounded to fine powder and pulverized at 200µm mesh size.

The prepared samples of 0.2 kg were packed in cylindrical polyethylene bottles. Afterward, they were completely sealed and stored for at least 4 weeks to maintain secular equilibrium between radium and its daughters.

2.2 Instrumentation and Calibration of NaI(Tl) Spectrometer

Radionuclides measurement was performed with a vertical 76 mm × 76 mm NaI(Tl) (Ortec model 905-4) scintillator detector connected to 1024 multichannel analyzer (MCA). The NaI(Tl) resolution FWHM (Full Width at Half Maximum) was 46.27 keV for ^{137}Cs peak. The gamma spectrometry system was calibrated using ^{60}Co, ^{137}Cs, and ^{152}Eu certified sources. For spectral analysis, a computer equipped with an acquisition cart and GammaVision software was used. To reduce the scattered and background radiation at the laboratory site, the central spectrometer was housed in a hollow Pb cylinder. The sample was vertically placed on the detector top, providing a high solid angle. The counting time was fixed at 24 hours for each sample. Moreover, the background activity was subtracted from each corresponding spectrum to get the net count. The specific activities of ^{232}Th, ^{238}U, and ^{40}K were measured by considering sample weight, detector efficiency, counting time, and gamma line intensity [12]. As reported in Table 1, different photopeaks and their intensities (I_γ) used for radioactivity measurements are tabulated.

TABLE 1. Gamma-ray emission corresponding to natural radioactive elements.

Radionuclides	Daughter	I_γ(%)	Associated energy Peak (keV)
^{232}Th	^{208}Tl	30.6	583.19
	^{208}Tl	35.85	2614.51
^{238}U	^{214}Bi	14.90	1120.3
	^{214}Bi	15.28	1764.49
^{40}K		10.66	1460.82

2.3 Calculation of Self-absorption Correction Factors

Due to the impact of the incident photon energy, and the chemical characteristics of the measurement geometry, the gamma-ray spectrometry technique requires the correction accounting for the fraction of the attenuated

photons inside the sample that are not detected by the spectrometer.

According to Dziri, the auto-absorption correction can be performed using either the setup proposed by Cutshall [11] or the Monte Carlo method. In the present study, the Cutshall transmission method was adopted. Figure 1 presents the experimental device adapted for gamma attenuation correction utilizing ^{152}Eu radioactive source, Pb collimators, and NaI(Tl) scintillator detector. The correction factor (C_{auto}) was defined by the ratio of the sample attenuation factor (F_{auto}) to the standard [11, 14].

The attenuation correction factor can be calculated through the equation:

$$C_{auto}(E) = \frac{F_{auto}^{sample}(E)}{F_{auto}^{standard}(E)} \quad (1)$$

where

$$F_{auto}(E) = \frac{1 - e^{-\mu(E)X}}{e^{-\mu(E)X}} \quad (2)$$

X (cm) and μ (cm^{-1}), are the thickness and the linear attenuation coefficient of the absorber material, respectively [14].

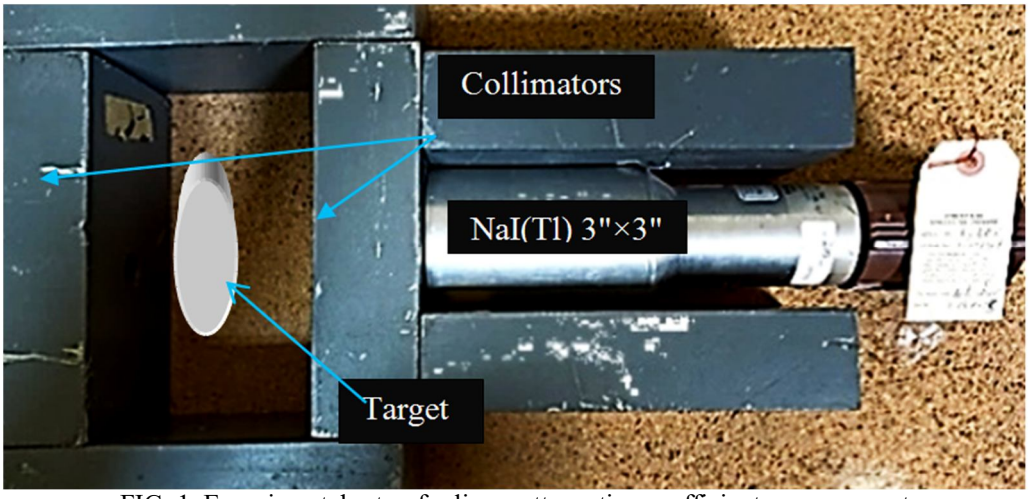

FIG. 1. Experimental setup for linear attenuation coefficient measurement.

3. Results and Discussion

3.1 Self-absorption Correction Factors and Elemental Analysis

Table 2 summarizes the densities and self-absorption correction factors of the studied materials at different energetic values. Based on the measured linear attenuation coefficient, an energetic fitting was applied to calculate the linear attenuation coefficient at 1460.8 keV for ^{40}K, 1120.3 and 1764.5 keV for ^{238}U, and 583.1 and 2614.6 keV for ^{232}Th. Later, the correction factors (F_{auto}) were calculated for each sample using Eq. (2). As reported in Table 2, it is very difficult to have a linear relationship between the correction factors, energies, and densities. However, it is not difficult to describe the dependency of correction factors by density, matrix composition, and incident photon energy. Moreover, it is observed that the three materials of tuff, concrete, and floor tile have the same density value, but there are varied values of C_{auto}. This variation may be due to the chemical composition of each material (See, Table 3). Additionally, it should be noted that the correction factor represents an energetic parameter added to correct the fraction of the attenuated gamma radiation inside the absorber.

TABLE 2. Densities and correction factors obtained by transmission method.

	Cement	Brick	Sand	Gravel	Tuff	Concrete	Floor tile
Density (g.cm^{-3})	3.03	2.55	2.53	2.65	2.56	2.56	2.56
C_{auto} *(581.1)*	0.87	0.86	0.82	0.86	0.81	0.85	0.82
C_{auto} *(1120.3)*	0.88	0.88	0.86	0.89	0.85	0.87	0.84
C_{auto} *(1460.8)*	0.89	0.89	0.88	0.89	0.89	0.91	0.88
C_{auto} *(1764.5)*	0.91	0.90	0.88	0.88	0.93	0.94	0.99
C_{auto} *(2614.6)*	0.97	0.94	0.80	0.76	0.98	0.98	0.99

TABLE 3. XRF for some construction materials.

	Oxide concentration (%)				
	Sand	Concrete	Cement	Gravel	Brick
B_2O_3	-	1.1907	1.5551	-	-
CO_2	13.841	55.1987	40.7576	58.8993	14.5546
Na_2O	0.0346	0.1248	0.0883	-	0.5902
MgO	0.2167	0.774	1.2411	1.0416	2.5093
Al_2O_3	1.4687	2.0961	2.9327	0.2071	11.8756
SO_3	0.0221	0.3746	-	0.03	3.3987
SiO_2	82.5829	11.8103	11.3851	0.7579	50.4724
P_2O_5	0.0204	0.0356	0.0695	0.0104	0.1828
K_2O	0.3215	0.2824	0.485	0.0211	1.6602
CaO	1.1643	27.2902	37.8041	38.931	9.6602
TiO_2	0.0612	0.0609	0.1316	-	0.5517
Cr_2O_3	-	0.007	0.0039	-	0.0258
MnO	-	0.019	0.022	-	0.0334
Fe_2O_3	-	0.699	1.487	0.0746	4.3309
NiO	-	0.0016	0.0039	-	0.0044
CuO	-	-	-	-	-
ZnO	-	0.0026	0.0028	0.003	0.0088
Rb_2O	-	0.0008	0.0013	-	0.0075
SrO	0.0021	0.0154	0.0488	0.0158	0.0396
ZrO_2	0.0063	0.0027	0.0042	-	0.0166
Nb_2O_5	-	-	-	-	0.0023
Y_2O_3	-	-	-	-	0.0023

To investigate the chemical composition of different construction materials, the wavelength dispersive XRF technique was used[1]. Table 3 compares the chemical compositions of the studied materials. A total of 22 elements were measured, namely, B_2O_3, CO_2, Na_2O, MgO, Al_2O_3, SO_3, SiO_2, P_2O_5, K_2O, CaO, TiO_2, Cr_2O_3, MnO, Fe_2O_3, NiO, CuO, ZnO, Rb_2O, SrO, ZrO_2, Nb_2O_5, and Y_2O_3.

The results indicate that a range of major elemental concentration was recorded for silica (SiO_2) (0.75-50.47%), lime (CaO) (1.16-38.03%), carbon dioxide (CO_2) (13.84-58.89%), and alumina (Al_2O_3) (0.207-11.87%). The variation in the elemental concentration can be explained by environmental factors, e.g., geological characteristics.

Based on the data presented in Table 1 and Table 3, Cutshall et al. demonstrated that the self-absorption phenomena are heavily influenced by the chemical composition and energetic range, especially at low energetic values where the photoelectric interaction is dominant. In our case, with higher energetic values, the dependency between these factors is slight, though not negligible.

[1]The XRF analysis was made in the CRAPC Expertise SPA, Bou Ismail, (w) Tipaza, Algeria.

Finally, the XRF results obtained in this study are in agreement with similar studies and meet the chemical criteria for construction design [22-23].

3.2 Natural Radioactivity Concentration of ^{238}U, ^{232}Th, ^{40}K

The assessed activities in the construction materials (in $Bq.kg^{-1}$) before and after self-absorption correction are shown in Fig. 2. It should be noted that the measured activities after the self-absorption correction are normalized by their corresponding correction factors (C_{auto}).

Moreover, it is obvious that the corrected activities are always higher than the non-corrected values. This discrepancy arises from the inclusion of the additional gamma radiation fraction. The mean of the activities' concentration (dry weight) is ranging from 15.18 ± 0.31 to 28.87 ± 0.37 $Bq.kg^{-1}$ for the ^{238}U series; from 16.35 ± 0.17 to 26.45 ± 0.12 $Bq.kg^{-1}$ for the ^{232}Th series; and from 362.28 ± 4.35 to 466.47 ± 5.34 $Bq.kg^{-1}$ for ^{40}K, where the major transmitter of ^{40}K is brick. The natural radionuclide concentrations are lower than the worldwide average of 30 $Bq.kg^{-1}$, 35 $Bq.kg^{-1}$, and 400 $Bq.kg^{-1}$ for ^{238}U, ^{232}Th, and ^{40}K, respectively [15].

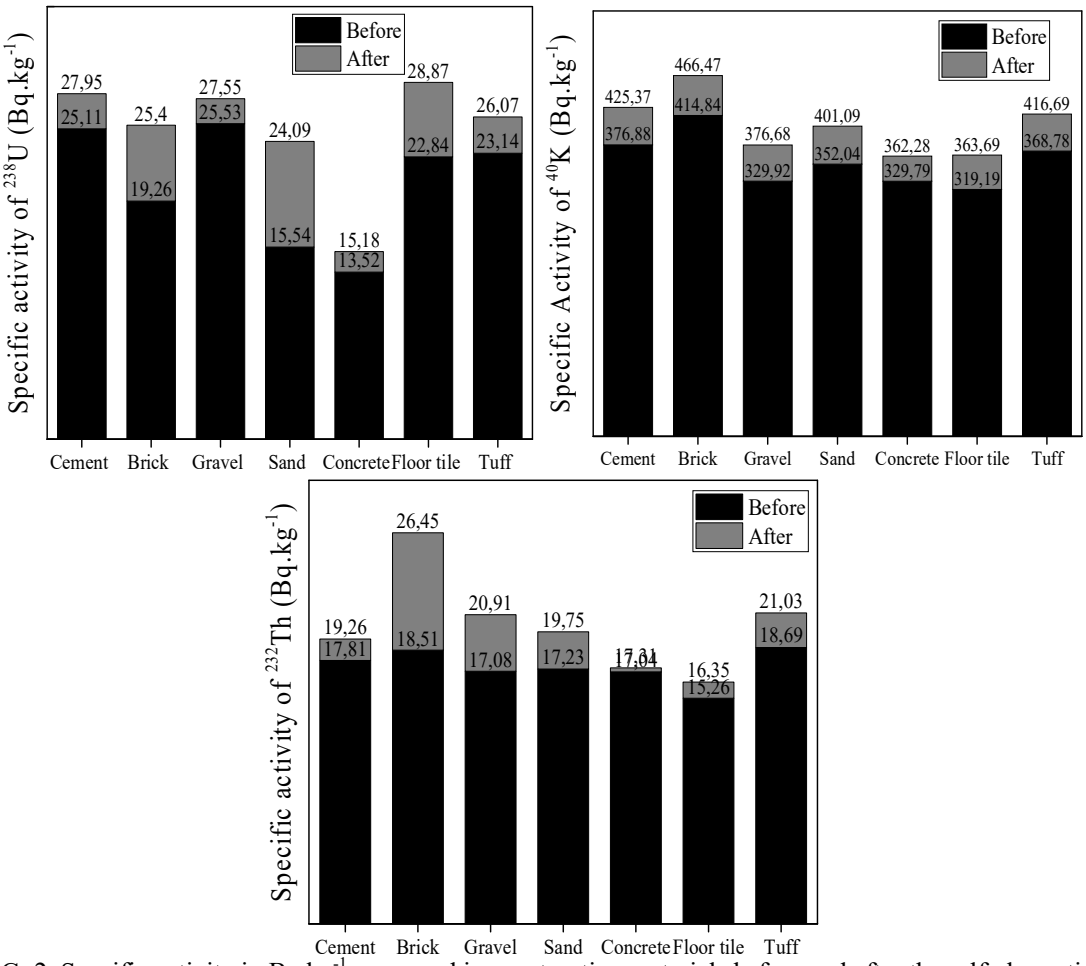

FIG. 2. Specific activity in Bq.kg^{-1} measured in construction materials before and after the self-absorption correction.

Table 4 presents the relative difference of specific activities before and after self-absorption correction. It seems that there is an increase in specific activities values (Bq.kg^{-1}): of 9.85 % to 14.17 % correspond to ^{40}K; of 1.58 % to 42.90 % correspond to ^{232}Th; 7.91 % to 55.02 % correspond to ^{238}U. The obtained results agree very well with the literature definition of C_{auto} factor.

To relate the mineralogical analysis with NORM concentration, Suresh et al. demonstrate that a correlation between the ^{226}Ra (^{238}U series), ^{228}Ra (^{232}Th series), ^{40}K, and minerals can be observed.

TABLE 4. Relative difference (%) on specific activities of ^{40}K, ^{232}Th, and ^{238}U.

	Cement	Brick	Sand	Gravel	Tuff	Concrete	Floor Tile
^{40}K	13.40	12.45	13.93	14.17	12.99	9.85	13.94
^{232}Th	8.14	42.90	14.63	22.42	12.52	1.58	7.14
^{238}U	11.31	31.87	55.02	7.91	12.66	12.28	26.40

3.3 Radiological Hazard Indices

3.3.1 Radium Equivalent Activity (Ra_{eq})

Due to the non-homogeneity distribution of natural radioactive elements in construction material, a single quantity defined by radium equivalent Ra_{eq} can be used to compare the associated radiation hazards level of ^{232}Th, ^{226}Ra, and ^{40}K. It can be calculated by the following equation [16]:

$$Ra_{eq} = A_{Ra} + 1.47A_{Th} + 0.077A_K \leq 370 \qquad (3)$$

where A_U, A_{Th}, and A_K are the specific activities of ^{226}Ra, ^{232}Th, and ^{40}K, respectively. According to UNSCEAR, 2000, the specific activity of ^{238}U is directly replaced by ^{226}Ra. Therefore, the radium equivalent values range between 67.84 Bq.kg^{-1} for concrete and 99.15 Bq.kg^{-1} for brick (See Table 5).

TABLE 5. Radium equivalent activity, external and internal hazard indexes, absorbed, and annual effective dose rate from construction materials.

Sample	Ra_{eq} *(Bq.kg^{-1})*	H_{ex}	H_{in}	*D(nGy.h^{-1})*	*E(mSv.y^{-1})*
Cement	88.28	0.16	0.31	42.28	0.21
Brick	99.15	0.18	0.34	47.26	0.23
Sand	83.22	0.15	0.30	37.72	0.19
Gravel	86.46	0.16	0.31	42.17	0.21
Tuff	88.25	0.16	0.31	42.13	0.21
Concrete	67.84	0.19	0.19	32.56	0.16
Floor Tile	80.26	0.15	0.30	38.38	0.19

In Fig. 3, the measured radium equivalent activities of some construction materials are compared with similar experimental data. For the Australian brick [16], the Ra_{eq} activity is almost double compared to our results. Whereas, the cement study conducted in Iran [17] shows a minimal quantity of the Ra_{eq} activity in comparison to existing literature. The Ra_{eq} values, of the present study, are comparable with similar studies and they are always lower than the worldwide limit corresponding to 370 Bq.kg^{-1}. Based on the disparities of the radium equivalent activities, the concentration variance can be due to background radiation level, environmental characteristics (geological formation), Radon concentration, etc.

Figure 4 shows the correlation degree between the radium equivalent activity (Bq.kg^{-1}) and NORM concentrations. Good correlation between the Ra_{eq}, ^{232}Th, and ^{40}K. Where the R square values were 0.71 and 0.74, respectively. The correlation coefficient of ^{238}U was 0.41. The significant disparities observed in the R square values between ^{228}Ra (^{232}Th series) and ^{226}Ra (^{238}U series) can potentially be attributed to variations in their respective half-life decay series.

3.2.1 External and Internal Hazard Indices

To evaluate the radiological and non-radiological hazards attributed to the radon carcinogenic, the parameters of an external H_{ex} corresponding to gamma radiation and internal H_{in} corresponding to alpha particle are used [15]. They are calculated using the following equations [1]:

$$H_{ex} = 0.0027A_{Ra} + 0.0037A_{Th} + 0.0002A_K \leq 1 \quad (4)$$

$$H_{in} = 0.0054A_{Ra} + 0.0039A_{Th} + 0.0002A_K \leq 1 \quad (5)$$

The average values of external and internal indices are presented in Table 5. The shown values are less than the unity.

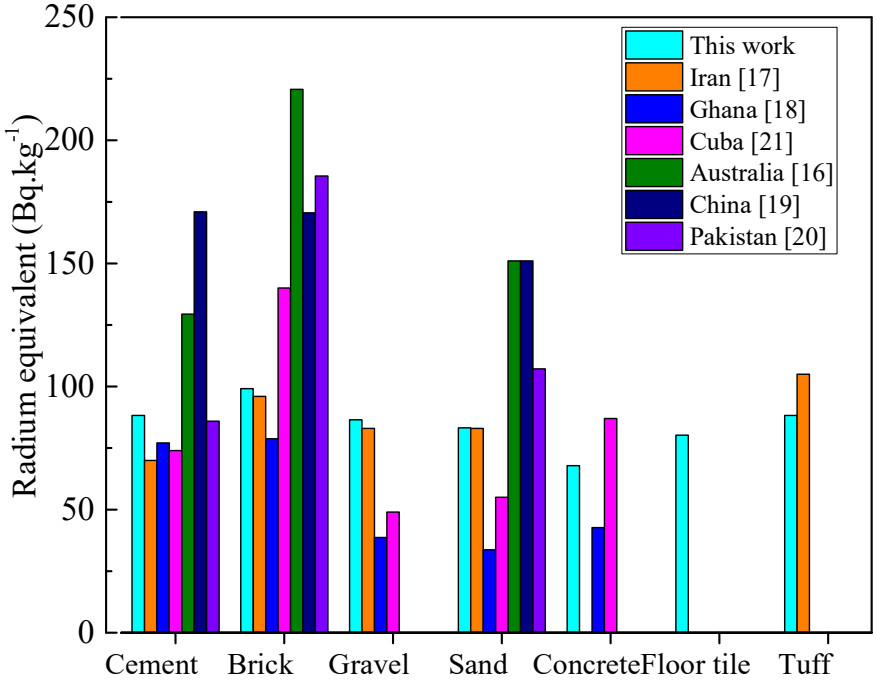

FIG. 3. Obtained Radium equivalent activity (Ra_{eq}) of construction materials in comparison to other counties.

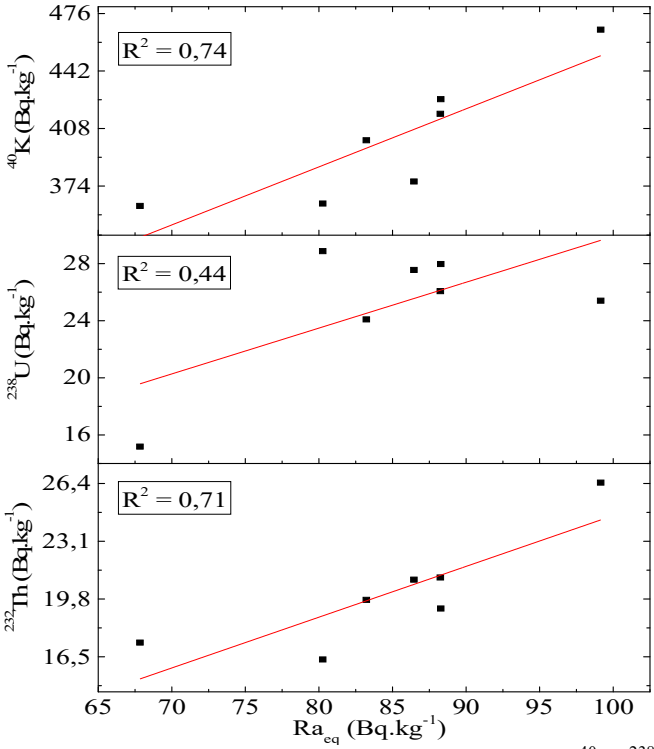

FIG. 4. Correlation factors between the radium equivalent activity, ^{40}K, ^{238}U, and ^{232}Th .

3.3.2 Absorbed Dose and Annual Effective Dose Rate in Air

The dosimetry parameter used for clinical and radiological characterization of external terrestrial gamma radiations is called the absorbed dose rate. It is calculated using the UNSCEAR formula [1]:

$$D\left(nGy.h^{-1}\right) = 0.462\,A_{Ra} + 0.604\,A_{Th} + 0.0417\,A_K \leq 55 \quad (6)$$

As described above, A_{Ra}, A_{Th}, and A_K are the specific activities of ^{226}Ra, ^{232}Th, and ^{40}K, respectively. The conversion coefficients 0.462, 0.604, and 0.0417 are used to pass from activity concentration to received absorbed air dose. The global average value of the absorbed dose rate is 55 nGy.h^{-1}[1].

The annual effective dose rate (AED) is directly calculated using the proposed UNSCEAR conversing factors. The annual effective dose rate due to the emitted gamma radiation of ^{238}U, ^{232}Th, and ^{40}K is given by the following equation:

$$E\left(mSv.y^{-1}\right) = D\left(nGy.h^{-1}\right) \times 8766 \times 0.8 \times 0.7 \times 10^{-6} \leq 1 \quad (7)$$

The annual estimated dose received by the collected geological sample is listed in Table 5. The maximum and the minimum values of the AED were recorded for the brick and the concrete sample as 0.23 and 0.16 mSv.y^{-1}, respectively. In the same table, it is reported that the AED values, for all samples, were always less than the upper limit corresponding to 1 mSv.y^{-1}.

4. Conclusion

The current study presents experimental data on natural terrestrial radionuclides ^{238}U, ^{232}Th, and ^{40}K, as well as their specific activities using a gamma spectrometry system. To correct the attenuated gamma radiations inside the absorber, the measured activities are normalized by the self-absorption correction factors. The results indicate that the variations in densities and chemical composition impact the measured activity, after the self-absorption, of 14.17 % for ^{40}K, 42.90 % for ^{232}Th, and 55.02 % for ^{238}U.

To review the radiological impact of the NORMs on human bodies, the radium equivalent activity, external and internal hazard indices, annual, and absorbed doses are determined. The radiological and mineralogical results show that the studied materials are acceptable for building design.

Furthermore, the X-ray fluorescence technique is employed to conduct mineralogical analysis. Out of the 22 elements detected, SiO_2, CaO, CO_2, and Al_2O_3 are identified as the primary constituents present in the construction materials.

This paper calls for additional research into self-absorption correction, specifically considering the chemical composition of the sample being analyzed.

References

[1] United Nations Scientific Committee on Effects of Atomic Radiation (UNSCEAR), "Exposures from Natural Radiation Sources", (U.N, New York U.S.A, 2000).

[2] El-Taher, A. and Althoyaib, S.S. Applied Radiation and Isotopes, 70 (2012) 1807.

[3] Nachab, A., Benjelloun, M., Nourreddine, A. and Pape, A. Physical and Chemical News, 7 (2002) 52.

[4] Knoll, G.F., "Radiation Detection and Measurement", Third edition, (John Willey and Sons Inc, New York, 2000).

[5] Nachab, A., Thesis (Doctorat in Sciences), l'Université Louis Pasteur - Strasbourg I, France et de l'Université Chouaïb Doukkali El Jadida, Maroc, 13 décembre (2003).

[6] Ali, H.T. and Khalil, J.K., Journal of Radiation Research and Applied Sciences, 10 (2017) 252.

[7] Ozyurt, O., Altinsoy, N., Karaaslan, Ş.J.E., Bora, A., Buyuk, B. and Erk, I., Radiation Physics and Chemistry, 144 (2018) 271.

[8] Bouisset, P., Lefèvre, O., Cagnat, X., Kerlau, G., Ugron, A. and Calmet, D., Nuclear Instruments and Methods in Physics Research, 437 (1999) 114.

[9] Medhat, M., Demir, N., Akar, T. and Gurler, U., Radiation Effects and Defects in Solids, 169 (2014) 706.

[10] Haddad, K. and Albyiat, R., Applied Radiation And Isotopes, 69 (2009) 1819.

[11] Cutshall, N.H., Larsen, I.L. and Olsen, C.R., Nuclear Instruments and Methods in Physics Research, 206 (1983) 309.

[12] International Atomic Energy Agency (IAEA), Technical reports: TECDOC 619, INSS 1011-4289, IAEA Publication, Vienna (1991).

[13] Dziri, S., Thesis (Doctorat in Sciences), Ecole doctorale de physique et chimie physique, Université de Strasbourg (2013).

[14] Battiston, G.A., Degetto, S., Gerbasi, R., Sbrignadello, G. and Tositti, L., Nuclear Instruments and Methods in Physics Research, 28 (1987) 438.

[15] United Nations Scientific Committee on the Effects of Atomic Radiation, (UNSCEAR), Report Volume I, Sources Report to the General Assembly Scientific Annexes A and B, sales No. E.10.XI.3 ISBN 978-92-1-142274-0, United Nations Publication, New York (2008).

[16] Beretka, J. and Mathew, P.J., Health Physics, 48 (1985) 87.

[17] Imani, M., Adelikhah, M., Shahrokhi, A. et al., Environmental Science and Pollution Research, 28 (2021) 41492.

[18] Otoo, F. et al., Scientific African, 1 (2018) e00009.

[19] Ziqiang, P., Yin, Y. and Mingqiang, G., Radiation Protection and Dosimetry, 24 (1988) 88.

[20] Tufail, M., Akhtar, N., Sabiha Javied. S. and Hamid. T., Journal of Radiation Protection, 27 (2007) 481.

[21] Brígido Flores, O., Montalván Estrada, A., Rosa Suárez, R., Tomás Zerquera, J. and Hernández Pérez, A., Journal of Environmental Radioactivity, 99 (2008) 1834.

[22] Dunuweera, S.P. and Rajapakse, R.M.G., Advances in Material Science and Engineering, (2018) ID 4158682.

[23] Mehboob, K., Alzahrani, Y.A., Fallatah, O., Qutub, M.M.T. and Younis, H., Arabian Journal for Science and Engineering, (2020).

[24] Suresh, G., Ramasamy, V., Meenakshisundaram,V., Venekatachalapathy, R. and Ponnusamy, V., Journal of Environmental Radioactivity, 102 (2012) 370.